NASA TM X-1615

NASA TECHNICAL MEMORANDUM

NASA TM X-1615

N68-28870
(ACCESSION NUMBER)
19
(PAGES)
TMX-1615
(NASA CR OR TMX OR AD NUMBER)
(THRU)
1
(CODE)
03
(CATEGORY)
FACILITY FORM 602

AERODYNAMIC PERFORMANCE OF A 4.59-INCH MODIFIED RADIAL-INFLOW TURBINE FOR A SINGLE-SHAFT BRAYTON CYCLE SPACE POWER SYSTEM

by Charles A. Wasserbauer and Milton G. Kofskey

Lewis Research Center
Cleveland, Ohio

NATIONAL AERONAUTICS AND SPACE ADMINISTRATION • WASHINGTON, D. C. • JULY 1968

NASA TM X-1615

AERODYNAMIC PERFORMANCE OF A 4.59-INCH MODIFIED RADIAL-INFLOW TURBINE FOR A SINGLE-SHAFT BRAYTON CYCLE SPACE POWER SYSTEM

By Charles A. Wasserbauer and Milton G. Kofskey

Lewis Research Center
Cleveland, Ohio

NATIONAL AERONAUTICS AND SPACE ADMINISTRATION

For sale by the Clearinghouse for Federal Scientific and Technical Information
Springfield, Virginia 22151 – CFSTI price $3.00

ABSTRACT

The turbine was modified to include a stator with 60 percent design throat area to be consistent with the single-shaft system requirements. Tests were conducted with argon at an inlet temperature of 560° R (311 K) and an inlet pressure of 6.0 psia (4.1 N/cm^2 abs). Performance results are presented in terms of equivalent specific work, torque, mass flow, and efficiency for a range of speeds from 0 to 110 percent of design.

STAR Category 03

AERODYNAMIC PERFORMANCE OF A 4.59-INCH MODIFIED RADIAL-INFLOW TURBINE FOR A SINGLE-SHAFT BRAYTON CYCLE SPACE POWER SYSTEM

by Charles A. Wasserbauer and Milton G. Kofskey

Lewis Research Center

SUMMARY

An experimental investigation of a radial-inflow turbine suitable for a single-shaft space power system was made. The turbine was modified from the original configuration to include a stator with a throat area 60 percent that of the original design and an exit diffuser in order to be consistent with the single-shaft system requirements. Tests were conducted at speeds ranging from 0 to 110 percent of equivalent design speed and at pressure ratios from 1.40 to 2.20 with argon as the working fluid.

The results of the investigation indicated that the static and total efficiencies, based on turbine-inlet to rotor-exit conditions, were 0.860 and 0.891, respectively. The equivalent mass flow, however, was 5.8 percent lower than that desired and was attributed to the stator flow area being smaller than that required for the attainment of design mass flow.

Turbine performance based on turbine-inlet to diffuser-exit conditions indicated static and total efficiencies of 0.875 and 0.880, respectively. These results indicate a 1 point drop in total efficiency and a 1.5 point increase in static efficiency through the diffuser.

Addition of the results of the variation of efficiency with specific speed of this turbine configuration to the results of the specific speed investigation of reference 3 showed that the efficiency does not drop off as rapidly with specific speed as was concluded in the reference study. The results indicated that total efficiencies in the 0.92 range could be obtained at high Reynolds numbers for specific speeds near 79 $(rpm)(ft^{3/4})/sec^{1/2}$ or 0.61 $(rad)(m^{3/2})(kg^{3/4})/(sec^{3/2})(J^{3/4})$. Calculation of velocity diagrams using experimental data at design operation showed the rotor to be operating in an off-design condition with incidence losses corresponding to approximately 1 point loss in total efficiency.

INTRODUCTION

The Brayton cycle space power system technology program at the Lewis Research Center includes the study of single- and two-shaft systems. A single-shaft system of current interest has a helium-xenon gas mixture as the working fluid and a power output of 2 to 10 kilowatts. Examination of system variables resulted in a specific speed value of 76 (rpm)$(ft^{3/4})/sec^{1/2}$ or 0.59 (rad)$(m^{3/2})(kg^{3/4})/(sec^{3/2})(J^{3/4})$ for the turbine with shaft speed of 36 000 rpm. The design combination of these variables and other operating conditions can be satisfied through modification of an existing high efficiency radial-inflow turbine. This turbine has a tip diameter of 4.59 inches (11.66 cm) and is a scale model of one designed to drive the compressor of a 10-kilowatt two-shaft argon space power system. References 1 to 3 define the turbine and report experimental performance over a range of Reynolds number with design geometry and over a range of specific speed obtained with four different stator blade row assemblies. The investigations of references 2 and 3 indicated that a total efficiency of 0.88 could be obtained for the single-shaft application with the stator closed down to approximately 60 percent of the original design stator throat area.

In view of the potential use of this turbine configuration, the turbine of réference 1 was modified with a redesigned stator blade row. In addition, an exit diffuser was designed to reduce the turbine exit velocity to a Mach number of 0.096. This is the design value for the single-shaft application.

The modified turbine was operated with cold argon at several values of speed and pressure ratio, with and without the diffuser. Performance measurements were made at each operating point to define speed, pressure ratio, torque, mass flow, efficiency, specific work, and blade-jet speed ratio. In addition, turbine exit radial surveys of pressure, temperature, and flow angle were made at equivalent design operating conditions.

The design operating conditions, turbine modifications, and experimental results obtained from the investigation of this modified turbine are presented herein.

SYMBOLS

H' isentropic specific work based on total pressure ratio, ft-lb/lb (J/g)

Δh specific work, Btu/lb (J/g)

N turbine speed, rpm (rad/sec)

N_s specific speed, $NQ^{1/2}/(H')^{3/4}$, (rpm)$(ft^{3/4})/sec^{1/2}$; (rad)$(m^{3/2})(kg^{3/4})/(sec^{3/2})(J^{3/4})$

p pressure, psia (N/cm^2 abs)

Q volume flow (based on rotor-exit conditions), ft^3/sec (m^3/sec)

Re Reynolds number, $w/\mu r_t$

r radius, ft (m)

U blade velocity, ft/sec (m/sec)

V absolute gas velocity, ft/sec (m/sec)

V_j ideal jet-speed corresponding to total- to static-pressure ratio across turbine, ft/sec (m/sec)

W relative gas velocity, ft/sec (m/sec)

w mass flow, lb/sec (kg/sec)

α absolute rotor exit gas flow angle measured from axial direction, deg

γ ratio of specific heats

δ ratio of inlet total pressure to U.S. standard sea-level pressure, p_1'/p^*

ϵ function of γ used in relating parameters to those using air inlet conditions at U.S. standard sea-level conditions, $\left(\frac{0.740}{\gamma}\right)\left(\frac{\gamma + 1}{2}\right)^{\gamma/(\gamma-1)}$

η_s static efficiency (based on inlet-total- to exit-static-pressure ratio)

η_t total efficiency (based on inlet-total- to exit-total-pressure ratio)

θ_{cr} squared ratio of critical velocity at turbine-inlet temperature to critical velocity at U.S. standard sea-level temperature, $(V_{cr}/V_{cr}^*)^2$

μ gas viscosity, lb/(ft)(sec); kg/(m)(sec)

ν blade-jet speed ratio, U_t/V_j

τ torque, in.-lb (N-m)

Subscripts:

cr condition corresponding to Mach number of unity

eq air equivalent (U.S. standard sea level)

t tip

u tangential component

w outer wall

1 station at turbine inlet (see fig. 2)

2 station at stator exit

3 station downstream of rotor exit when straight exit section was used

4 station at diffuser exit

Superscripts:

' absolute total state

* U. S. standard sea-level conditions (temperature, 518.67° R or 288.15 K; pressure, 14.70 psia or 10.13 N/cm^2)

TURBINE DESCRIPTION

The 4.59-inch tip-diameter radial-inflow turbine described in reference 1 was used for this investigation. Air equivalent design values corresponding to the modified turbine for single-shaft operation as well as the original turbine design values are as follows:

	Modified turbine	Original turbine
Rotative speed, $N/\sqrt{\theta_{cr}}$, rpm (rad/sec)	29 680 (3108.1)	29 550 (3094.5)
Mass flow, $w\epsilon\sqrt{\theta_{cr}}/\delta$, lb/sec (kg/sec)	0.486 (0.220)	0.616 (0.279)
Total- to total-pressure ratio		
Rotor exit, $(p_1'/p_3')_{eq}$	-------------	1.496
Flange to flange, $(p_1'/p_4')_{eq}$	1.658	-------------
Total- to static-pressure ratio		
Rotor exit, $(p_1'/p_3)_{eq}$	-------------	1.540
Flange to flange, $(p_1'/p_4)_{eq}$	1.669	-------------
Mach number		
Rotor exit	-------------	0.203
Diffuser exit	0.096	-------------

As mentioned in the INTRODUCTION, the turbine of reference 1 was modified by incorporating a stator blade row with a throat area closed down to approximately 60 percent of the original design value.

Optimum performance would not be expected with this modified turbine since the rotor would be operating at off-design conditions. The velocity diagrams would be considerably different than the velocity diagrams for which the rotor was designed. The influence of off-design operation of the rotor on turbine performance will be discussed in the RESULTS AND DISCUSSION section.

Figure 1 shows the turbine stator, rotor, and exit diffuser used in the investigation.

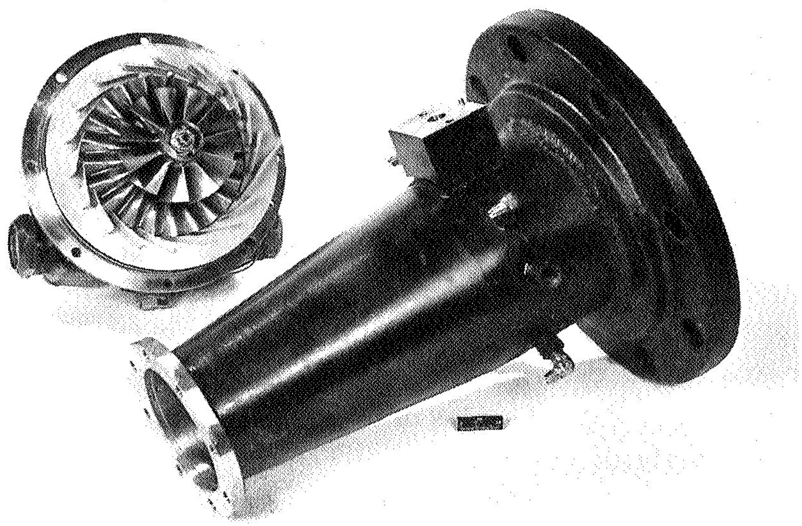

C-67-4269

Figure 1. - Turbine rotor, stator, and exit diffuser.

The stator has 18 blades, one of which had an elongated leading edge to block the flow from entering the small area end of the inlet scroll.

The rotor has 11 blades and 11 splitter vanes. These splitter vanes are used over the initial third of the rotor, thereby increasing the solidity in this region. The resultant decrease in loading was required at the hub to prevent low blade pressure-surface gas velocities.

The exit diffuser is conical and the area varies from 8.56 square inches (55.23 sq cm) at the inlet to 20.03 square inches (129.23 sq cm) at the exit. This variation in area with axial distance results in a half angle of diffusion of about $6^{\circ}27'$.

APPARATUS, INSTRUMENTATION, AND METHODS

The test facility, instrumentation, and method of calculating performance parameters were similar to those described in reference 1. Essentially the apparatus consisted of the research turbine, an airbrake dynamometer to absorb and measure the power output of the turbine, and an inlet and exhaust piping system with flow controls. Pressurized argon was used as the driving fluid for the turbine. The argon was piped into the turbine through an electric heater, a filter, a mass-flow measuring station that consisted of a calibrated flat-plate orifice, and a remotely controlled pressure-regulating valve. The gas, after expanding through the turbine, was passed through a remotely controlled exhaust valve and into the laboratory low-pressure exhaust system.

With a fixed inlet pressure, the remotely operated valve in the exhaust line was used to obtain the desired pressure ratio across the turbine.

The airbrake dynamometer, which was cradle mounted to measure torque, absorbed and measured the power output of the turbine and, at the same time, controlled the speed. The force on the torque arm was measured with a commercial strain-gage load cell. The rotational speed was measured with an electronic counter in conjunction with a magnetic pickup and a shaft-mounted gear.

Two series of tests were made. In the first series, a straight annular section was used at the rotor exit for the determination of performance based on turbine-inlet and rotor-exit conditions. The second series of tests were made with the exit diffuser for the overall or flange-to-flange performance.

The measuring stations are shown in figure 2. Briefly, overall performance (turbine inlet to diffuser exit) was based on measurements taken at stations 1 and 4. Turbine performance was also determined by measurements taken at stations 1 and 3 (turbine inlet to rotor exit). The following instrumentation was located at the turbine inlet (station 1): four static pressure taps, a total pressure probe, and a total temperature rake consisting of three thermocouples. The total pressure probe was used for setting and monitoring the turbine-inlet pressure. At the rotor exit (station 3), the instrumentation consisted of six static pressure taps, three each at the inner and outer walls, and a self-alining probe for flow angle, total temperature, and total pressure measurement. At the diffuser exit (station 4), the instrumentation consisted of four static pressure taps and a self-alining probe for flow angle, total pressure, and total temperature measurements. In addition to the instrumentation at these stations, one static pressure tap was located in the plane of the stator blade trailing edge at the midchannel point (station 2).

Performance data were taken at nominal inlet total conditions of 560° R (311 K) and 6.0 pounds per square inch absolute (4.1 N/cm^2 abs) which corresponds to the Reynolds number encountered in actual operation. Data were obtained over a range of total- to static-pressure ratios from 1.40 to 2.20 and a speed range from 0 to 110 percent of equivalent design speed.

Friction torque of the turbine bearings and seals was obtained by measuring the amount of torque required to rotate the shaft and rotor over the range of speeds covered in the investigation. In order to minimize windage losses, air was evacuated from the turbine during the friction tests. A friction torque value of 0.69 inch-pound (0.078 N-m), which corresponds to approximately 8 percent of turbine torque obtained at design-point operation. Friction torque was added to the shaft torque when turbine efficiency was determined.

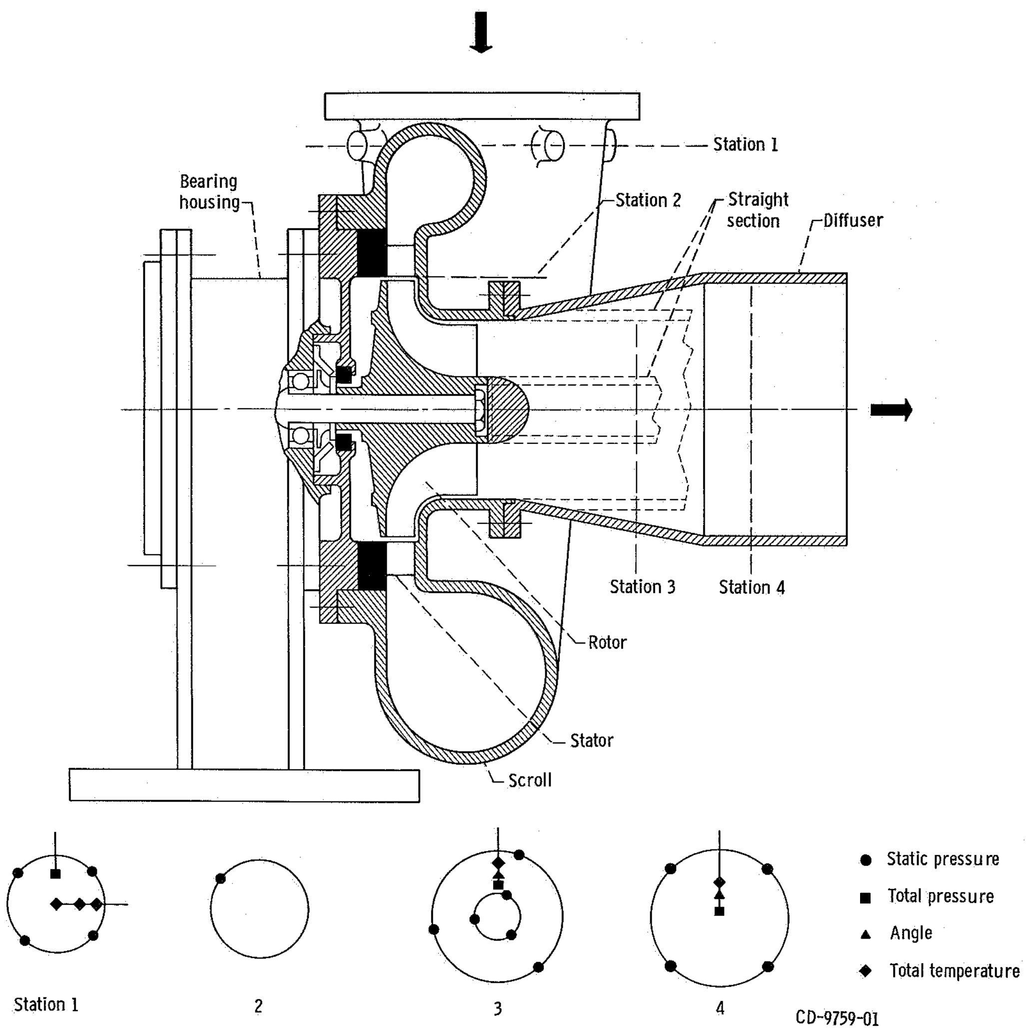

Figure 2. - Turbine test section and instrumentation.

RESULTS AND DISCUSSION

From the results of the tests of the turbine with the diffuser at the overall single-shaft design-point condition, rotor-exit conditions and, hence, blade-jet speed ratio at design-point operation could be determined. These conditions together with the pertinent single-shaft design-point performance results are shown in table I.

The results of this investigation are presented in two sections. The first section describes the performance of the turbine based on conditions at both the rotor and diffuser exit. The second section then presents an interpretation of the results by a comparison of the velocity diagrams for which the turbine was designed to the off-design velocity diagrams as imposed by the single-shaft overall design operating conditions. Since the stator configuration may be considered as an additional configuration of the specific speed investigation of reference 3, the variation of efficiency with specific speed for all stator configurations will also be discussed.

TABLE I. - EXPERIMENTAL PERFORMANCE VALUES

Total efficiency (based on rotor-exit conditions), $\eta_{t,1-3}$	0.891
Static efficiency (based on rotor-exit conditions), $\eta_{s,1-3}$	0.860
Overall total efficiency, $\eta_{t,1-4}$	0.880
Overall static efficiency, $\eta_{s,1-4}$	0.875
Equivalent mass flow, $w\epsilon\sqrt{\theta_{cr}}/\delta$, lb/sec (kg/sec)	0.458 (0.208)
Equivalent specific work, $\Delta h/\theta_{cr}$, Btu/lb (J/g)	15.00 (34.92)
Equivalent torque, $\tau\epsilon/\delta$, in.-lb (N-m)	20.4 (2.3)
Equivalent turbine-inlet-total- to rotor-exit-static-pressure ratio, $(p_1'/p_3)_{eq}$	1.695
Blade-jet speed ratio, ν	0.636

Performance Results

Figure 3 shows the variation of equivalent mass flow with pressure ratio for lines of constant speed. At design-point operation, the equivalent mass flow was 0.458 pound per second (0.208 kg/sec). This is about 5.8 percent lower than the design value of 0.486 pound per second (0.220 kg/sec). The deficiency in mass flow results from the stator throat area being smaller than that required for the attainment of design mass flow. The adjustment of 0.5° in stator blade setting angle would give design mass flow without any significant change in efficiency.

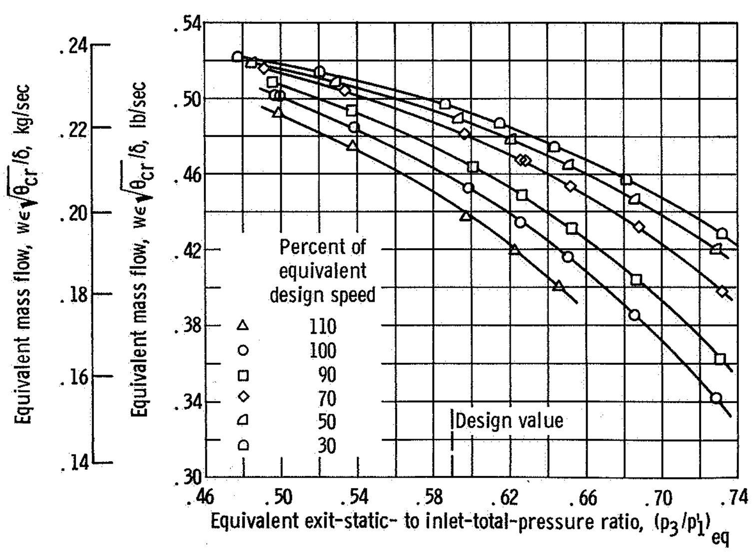

Figure 3. - Variation of mass flow with pressure ratio for lines of constant speed.

Figure 4 shows the variation of equivalent specific work $\Delta h/\theta_{cr}$ with total- to static-pressure ratio for lines of constant speed. The specific work was 15.00 Btu per pound (34.92 J/g) at design-point operation. It may be noted that, at the equivalent design pressure ratio (1.695), the turbine work varied by less than 2 percent as the speed was varied from 90 to 110 percent. This indicates that, at this pressure ratio, the tur-

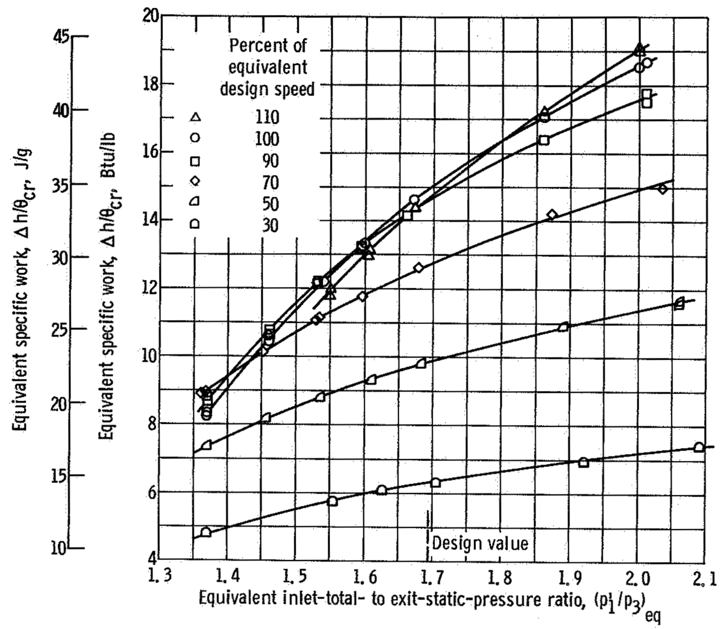

Figure 4. - Variation of specific work with pressure ratio and speed.

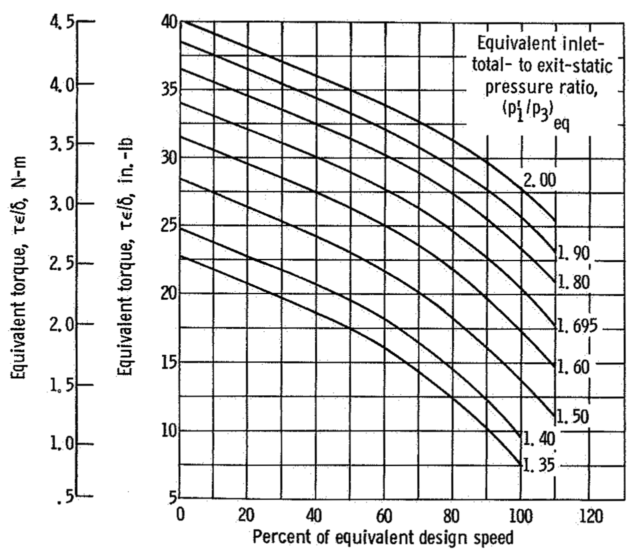

Figure 5. - Variation of torque with speed and pressure ratio.

bine was operating in the region where peak efficiency occurs. The figure also shows that limiting loading was not reached over the pressure ratio range investigated.

The variation of torque $\tau\epsilon/\delta$ with speed for lines of constant pressure ratio $\left(p_1'/p_3\right)_{eq}$ is shown in figure 5. The torque at design-point operation was 20.4 inch-pounds (2.3 N-m). The figure also shows that zero speed torque, at design pressure ratio, is 34 inch-pounds (3.8 N-m) which is 1.7 times the value obtained at design speed and pressure ratio. This ratio and the trends of the curves are consistant with the results obtained from other radial flow turbines.

Figure 6 shows the efficiencies of the turbine, based on measurements taken at the

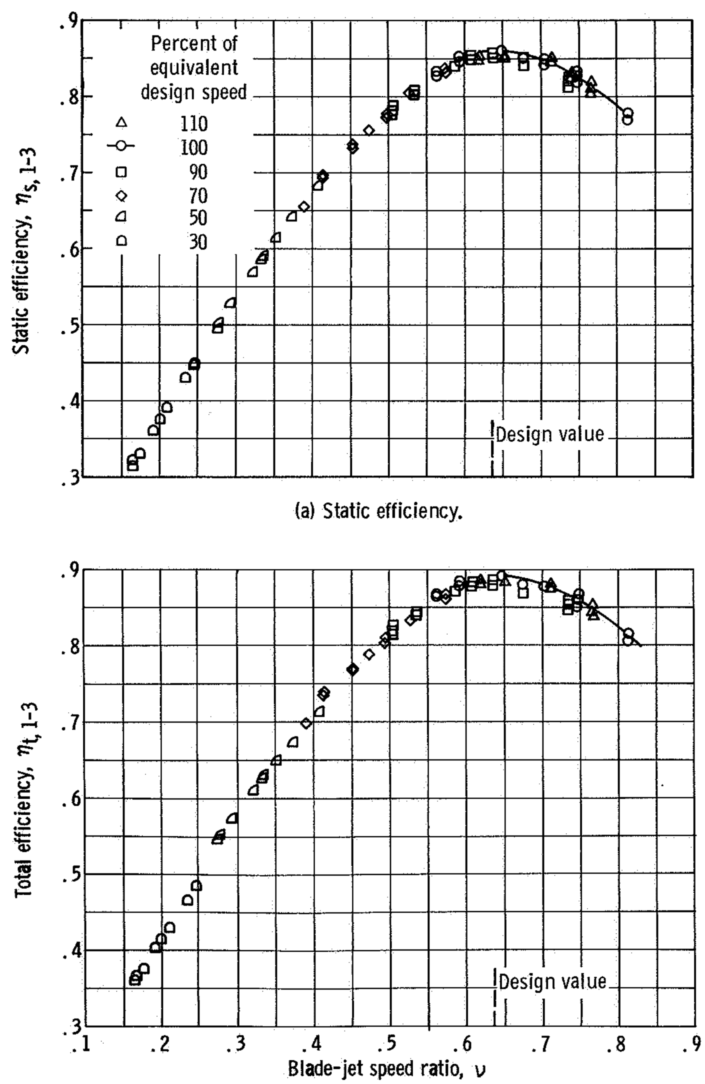

(a) Static efficiency.

(b) Total efficiency.

Figure 6. - Variation of static and total efficiency with blade-jet speed ratio (based on rotor-exit conditions).

turbine inlet and rotor exit, in terms of static and total efficiencies. The curve shown in the figure represents the variation of efficiency for design speed and over the range of pressure ratios investigated. Figure 6(a) shows a static efficiency value of 0.860 was obtained at design speed and at design blade-jet speed ratio of 0.636. Figure 6(b) shows that a total efficiency value of 0.891 was obtained at design speed and design blade-jet speed ratio indicating that 3 points in efficiency were involved in exit kinetic energy.

Figure 7 shows the overall turbine efficiencies including the exit diffuser. Figure 7(a) shows that a static efficiency of 0.875 was obtained at design speed and design

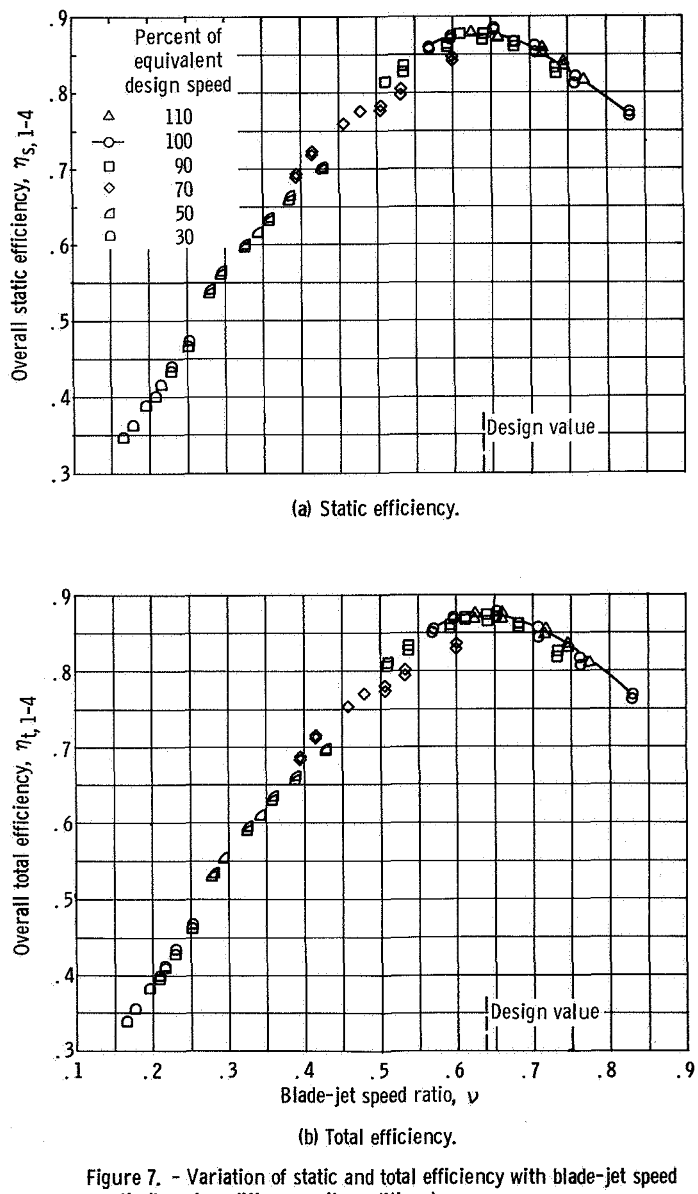

Figure 7. - Variation of static and total efficiency with blade-jet speed ratio (based on diffuser-exit conditions).

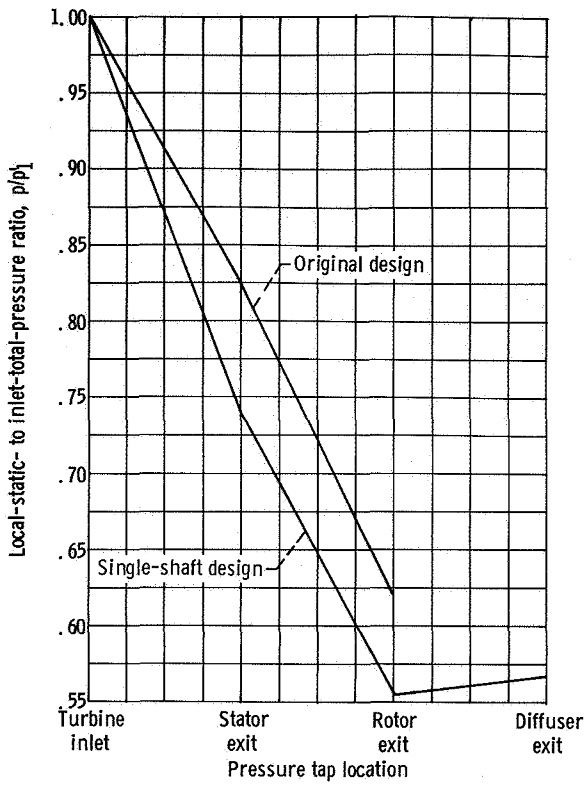

Figure 8. - Experimental variation of static pressure through two turbine configurations at their equivalent design-point operation.

blade-jet speed ratio. Figure 7(b) shows that the associated total efficiency was 0.880. Thus, the inclusion of the diffuser resulted in a 1.5 point increase in static efficiency and a 1 point decrease in total efficiency as compared with the efficiencies obtained from turbine inlet to rotor exit.

Figure 8 shows the static pressure variation through the turbine and diffuser for equivalent design speed and design pressure ratio. The static pressure variation obtained from the tests with the original 100 percent stator setting is also shown for comparison purposes. The figure shows that, the single-shaft design, there was considerably more stator reaction. Rotor reaction, however, was about the same for both designs. Static pressure recovery through the diffuser (rotor exit to diffuser exit) is also shown in the figure. The ratio of diffuser static pressure recovery to the diffuser inlet impact pressure was approximately 0.6, which is consistant with that obtained for diffusers of this type.

The results of a radial survey of rotor exit total pressure, total temperature, and flow angle taken at equivalent design speed and pressure ratio are shown in figure 9. Figure 9(a) presents the variation in rotor exit flow angle with radius ratio. Overturning, as evidenced by the negative angle, was obtained over approximately one-half of the pas-

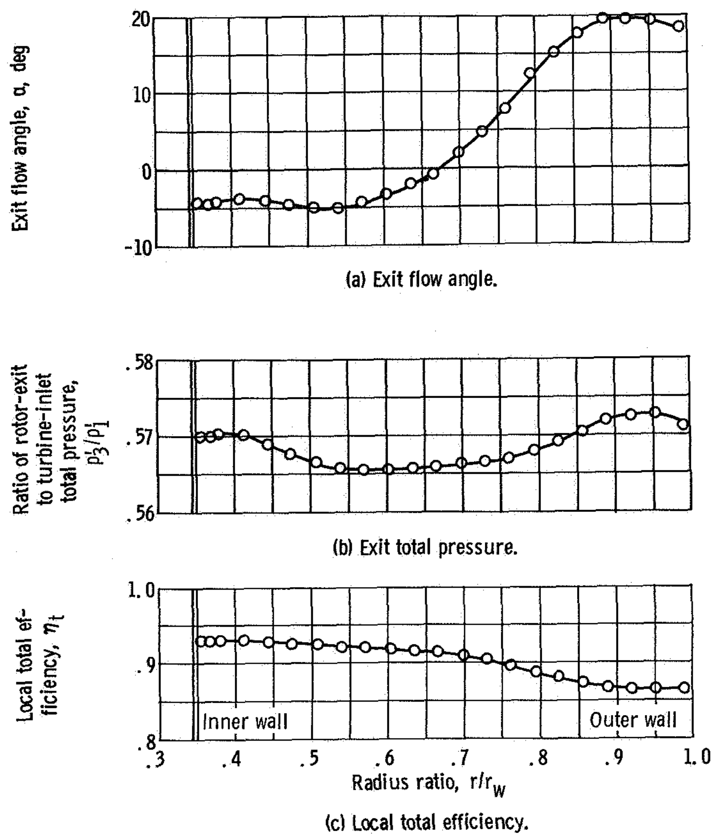

Figure 9. - Variation of rotor-exit flow angle, total pressure, and local total efficiency with radius ratio at design-point operation.

sage, and underturning over the remaining part of the passage near the outer wall. Figure 9(b) shows the variation of exit total pressure with radius ratio. As can be seen from the figure, there were minor variations in total pressure over the entire passage height.

Local values of total efficiency were calculated on the basis of the change in tangential momentum through the rotor and the radial distribution of total pressure at the rotor exit. The values of local total efficiency are shown as a function of radius ratio in figure 9(c). There is a maximum variation of approximately 6.5 percentage points in efficiency from hub to outer wall with the lowest efficiencies occurring near the outer wall.

Specific Speed and Velocity Diagram Considerations

Having established the pertinent performance characteristics of the turbine it is now possible to determine how this turbine configuration, designed for a specific speed of 76 $(\mathrm{rpm})(\mathrm{ft}^{3/4})/\mathrm{sec}^{1/2}$ or 0.59 $(\mathrm{rad})(\mathrm{m}^{3/2})(\mathrm{kg}^{3/4})/(\mathrm{sec}^{3/2})(\mathrm{J}^{3/4})$, fits in with the specific speed investigation of reference 3. In addition, since this turbine operated at a lower blade-jet speed ratio than normally used, it was of interest to determine the design-point operating velocity diagrams in order to determine what the penalty, in terms of efficiency, might be when operating the rotor at off-design conditions.

Since the 60 percent stator configuration may be considered as an additional configuration in the specific speed range of reference 3, the variation of efficiency with specific speed for the four stator configurations of this reference is shown with the results obtained with the 60 percent stator configuration. The efficiencies of this investigation were adjusted for Reynolds number since the reference investigation was made at a higher nominal Reynolds number of 277 000. The adjustment in efficiencies was made in accordance with the results of the Reynolds number investigation of this 4. 59-inch turbine as reported in reference 2. Figure 10 shows the variation of efficiency with specific speed for the five stator configurations. The 125, 100, 75, and 50 percent stator configuration efficiencies were obtained from reference 3 while the 60 percent configuration

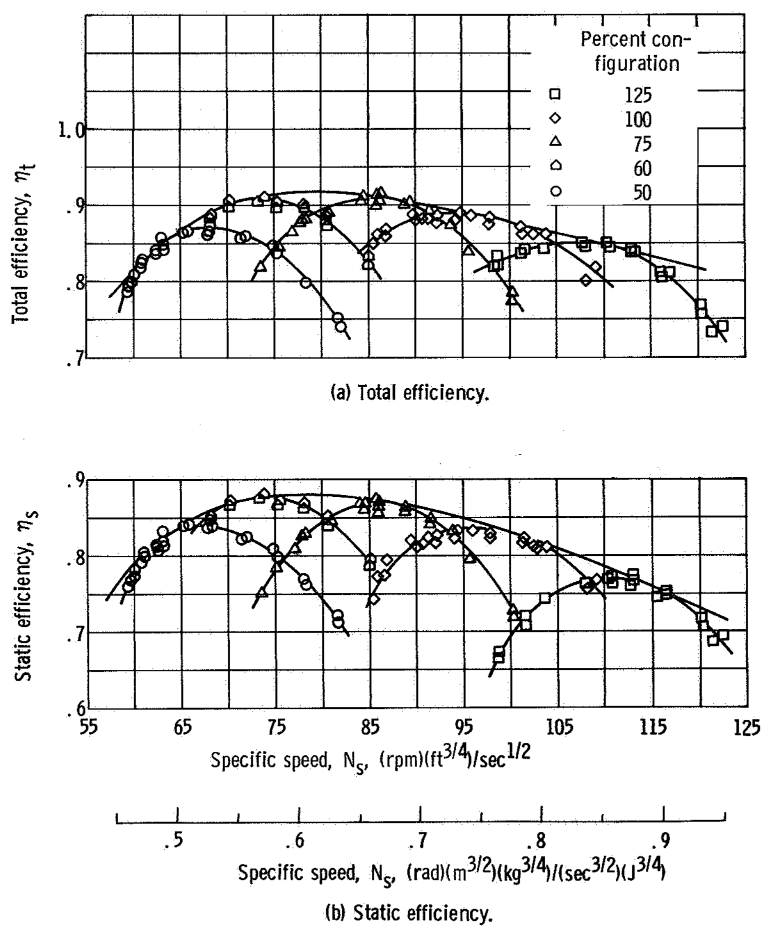

Figure 10. - Variation of efficiency with specific speed at equivalent design speed (Reynolds number, 277 000).

efficiencies were obtained from this investigation. Figure 10(a) shows the variation of total efficiency with specific speed with the heavy curve representing the envelope of the efficiency curves for all configurations. The figure indicates that the highest total efficiency value of 0.92 could be obtained at specific speeds near 79 $(rpm)(ft^{3/4})/sec^{1/2}$ or 0.61 $(rad)(m^{3/2})(kg^{3/4})/(sec^{3/2})(J^{3/4})$. Reference 3 stated that a maximum total efficiency value of 0.91 was obtained at a specific speed of approximately 86 $(rpm)(ft^{3/4})/sec^{1/2}$ or 0.67 $(rad)(m^{3/2})(kg^{3/4})/(sec^{3/2})(J^{3/4})$. Application of the results of the 60 percent stator configuration indicates that the efficiency does not drop off as rapidly with specific speed as was concluded in reference 3.

Figure 10(b) shows the variation of static efficiency with speed, as in the case for total efficiency, addition of the 60 percent stator configuration data indicates that the efficiency does not drop off as rapidly as was indicated by the lower plot of figure 6 in the reference report. Figure 10(b) indicates the highest static efficiency value of 0.88 could be obtained at a specific speed of approximately 75 $(rpm)(ft^{3/4})/sec^{1/2}$ or 0.58 $(rad)(m^{3/2})(kg^{3/4})/(sec^{3/2})(J^{3/4})$.

As mentioned previously, the turbine rotor was operating in an off-design condition for the single-shaft application. In order to determine the off-design operation effects on performance, velocity diagrams were calculated from experimental data obtained at design-point operation. Figure 11 shows these calculated velocity diagrams at the stator

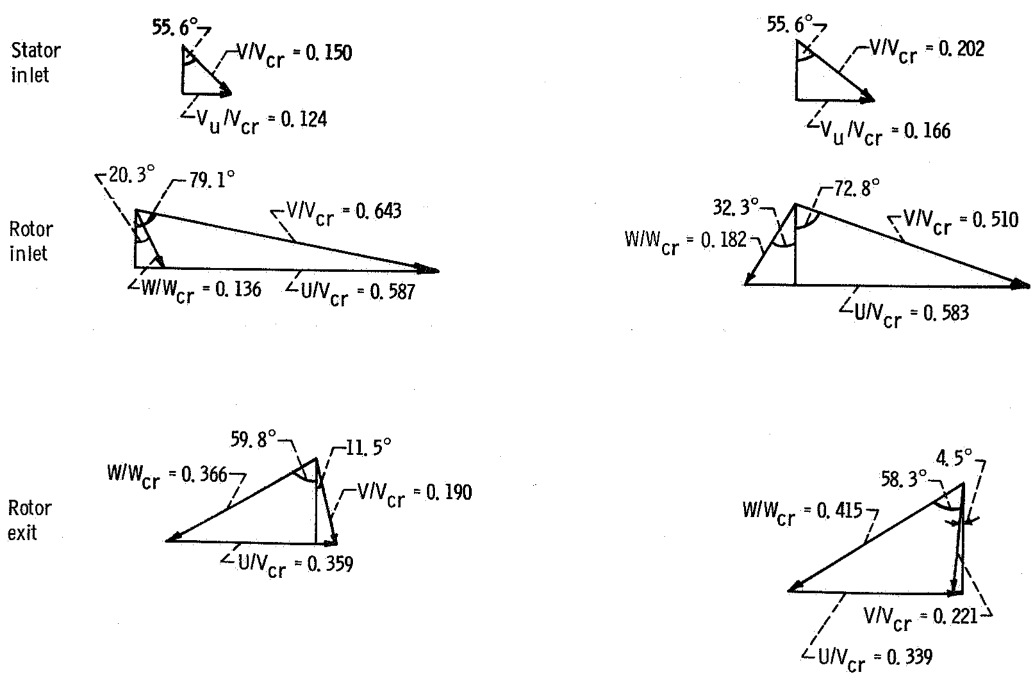

(a) Single-shaft, 60 percent stator configuration.

(b) Original 100 percent stator configuration.

Figure 11. - Comparison of turbine velocity diagrams at respective equivalent design speeds and pressure ratios. Radius ratio, r/r_w = 0.772.

entrance and exit and at a rotor exit radius 0.772 that of the outer wall. The velocity diagrams for the 100 percent stator configuration were also calculated from experimental data and are also shown. The figure shows that there is considerable difference in rotor relative inlet angle between the two configurations. The original configuration has a relative inlet angle of 32.3°, while the modified turbine has a relative inlet angle of 20.3°. Optimum relative angle for the modified turbine was calculated to be 23.6°. This gives an incidence angle of 43.9° for the modified turbine. If it was assumed that the component of the relative inlet flow normal to the incidence angle is lost, correspondingly, about 1 point in total efficiency was calculated to be lost because of this off-design operating condition.

SUMMARY OF RESULTS

The results of the experimental investigation of a 4.59-inch (11.66-cm) tip-diameter radial-inflow turbine have been presented herein. This turbine was modified from that used in a reference investigation to include a redesigned stator blade row and an exit diffuser which made it suitable for a single-shaft space power application. The results of this investigation are summarized as follows:

1. An equivalent specific work of 15.00 Btu per pound (34.92 J/g) was obtained at design operation. The associated static and total efficiencies (based on turbine-inlet to rotor-exit conditions) were 0.860 and 0.891, respectively.

2. Performance of the turbine based on turbine-inlet to diffuser-exit conditions indicated static and total efficiencies of 0.875 and 0.880, respectively. These results indicate a drop of 1 point in total efficiency within the diffuser. There was a corresponding 1.5 point increase in static efficiency through the diffuser.

3. The equivalent mass flow was 0.458 pound per second (0.208 kg/sec) at design operation. This value is 5.8 percent lower than desired and resulted from the stator throat area being smaller than that required to obtain design flow.

4. Addition of the 60 percent stator configuration data to a reference specific speed investigation showed that the efficiency does not drop off as rapidly with specific speed as was concluded in the reference. The results also indicated that at high Reynolds numbers, total efficiencies in the 0.92 range could be obtained for specific speeds near 79 $(\mathrm{rpm})(\mathrm{ft}^{3/4})/\mathrm{sec}^{1/2}$ or 0.61 $(\mathrm{rad})(\mathrm{m}^{3/2})(\mathrm{kg}^{3/4})/(\mathrm{sec}^{3/2})(\mathrm{J}^{3/4})$.

5. The turbine was found to be operating in an off-design condition under the single-

shaft application requirements resulting in approximately 1 point loss in total efficiency due to rotor incidence.

Lewis Research Center,
National Aeronautics and Space Administration,
Cleveland, Ohio, April 9, 1968,
120-27-03-56-22.

REFERENCES

1. Wasserbauer, Charles A.; Kofskey, Milton G.; and Nusbaum, William J.: Cold Performance Evaluation of a 4.59-Inch Radial-Inflow Turbine Designed for a Brayton-Cycle Space Power System. NASA TN D-3260, 1966.
2. Nusbaum, William J.; and Wasserbauer, Charles A.: Experimental Performance Evaluation of a 4.59-Inch Radial-Inflow Turbine Over a Range of Reynolds Number. NASA TN D-3835, 1967.
3. Kofskey, Milton G.; and Wasserbauer, Charles A.: Experimental Performance Evaluation of a Radial-Inflow Turbine over a Range of Specific Speeds. NASA TN D-3742, 1966.

"The aeronautical and space activities of the United States shall be conducted so as to contribute . . . to the expansion of human knowledge of phenomena in the atmosphere and space. The Administration shall provide for the widest practicable and appropriate dissemination of information concerning its activities and the results thereof."

—NATIONAL AERONAUTICS AND SPACE ACT OF 1958

NASA SCIENTIFIC AND TECHNICAL PUBLICATIONS

TECHNICAL REPORTS: Scientific and technical information considered important, complete, and a lasting contribution to existing knowledge.

TECHNICAL NOTES: Information less broad in scope but nevertheless of importance as a contribution to existing knowledge.

TECHNICAL MEMORANDUMS: Information receiving limited distribution because of preliminary data, security classification, or other reasons.

CONTRACTOR REPORTS: Scientific and technical information generated under a NASA contract or grant and considered an important contribution to existing knowledge.

TECHNICAL TRANSLATIONS: Information published in a foreign language considered to merit NASA distribution in English.

SPECIAL PUBLICATIONS: Information derived from or of value to NASA activities. Publications include conference proceedings, monographs, data compilations, handbooks, sourcebooks, and special bibliographies.

TECHNOLOGY UTILIZATION PUBLICATIONS: Information on technology used by NASA that may be of particular interest in commercial and other non-aerospace applications. Publications include Tech Briefs, Technology Utilization Reports and Notes, and Technology Surveys.

Details on the availability of these publications may be obtained from:

SCIENTIFIC AND TECHNICAL INFORMATION DIVISION

NATIONAL AERONAUTICS AND SPACE ADMINISTRATION

Washington, D.C. 20546